Removal of trapped charge in selenium detectors

Denny Lee[1] and Andrew D.A. Maidment[2]
Directxray Digital Imaging Technology LLC[1], West Chester, PA USA
Department of Radiology[2], University of Pennsylvania, Philadelphia, PA, USA
dlee@directxray.com, Andrew.Maidment@uphs.upenn.edu

ABSTRACT

Flat panel selenium detectors (1) have been commercially available since 1998 (2). The MTF of these detectors can approach the theoretical SINC function for the pixel size (3). Detectors can be designed with selenium thickness suitable for absorption of the range of x-ray energy for the modality (4, 5). For higher energy x rays, the thickness of the selenium layer can be increased without greatly degrading the spatial resolution. The non-spreading nature of the signal allows the detector to detect very weak x-ray signal in the vicinity of strong signal. Selenium detectors can therefore be designed to produce very high dynamic range images when needed. However, as a photo-conducting material, selenium also comes with some less than ideal properties. For example, charge trapping, long settling time for with bias electric field, and interface charge injection (6). These adverse properties must be included in detector design for optimal performance in each application. This paper describes a novel method for interfacial charge removal using lateral conductivity of selenium.

1. IMAGING WITH SELENIUM

Amorphous selenium was first used as a photo-conducting material in the late 1930's for electro-photography. In the last thirty years, its application has been extended to the area of medical imaging and used as an x-ray to image charge converter. All through these years, even after numerous talented researchers have devoted extensive effort to understand this material, many of its electrical and imaging properties are still not completely understood. With the absorption of an energetic x-ray photon (mostly via the photoelectric effect), electron-hole pairs (ehp's) are generated. For x-ray energy in the medical imaging range, (less than 150 keV), the range of the primary energetic photoelectron is in the order of 10 to 20 microns. Along its track, more electron hole pairs are generated from the collision of the primary electron with other selenium atoms. Under a bias electric field, a fraction of the ehp's are separated and move along the bias electric field with the rest either being recombined (neutralized) or remaining closely bound. The fraction of ehp's separated is proportional to the strength of the bias electric field. The ratio between the number of ehp's separated and the number able to move along the field line to the primary x-ray energy is called the work function (W). At a bias field of 10 volts per micron, the typical W is approximately 50 eV/ehp for amorphous selenium; i.e. on average, it requires 50 eV of deposited x-ray energy to generate one electron hole pair that can travel along a field line and contribute to the image signal (7). This energy is relatively high in comparison to most other photo-conducting materials, which most typically only require 2.8 times the band gap energy to generate an electron hole pair.

Furthermore, while the separated electrons and holes are moving along the bias electric field line, they can be trapped by local potential well, or by lattice defects. Depending on the depth of the potential well, some trapped charges acquire thermal energy and resume their movement after a brief moment. The deeply trapped charge may remain trapped for a long time (on the order of hours to years) if no de-trapping energy is available. The delayed action of trapping and de-trapping charge may cause image lag, image ghosting, and/or contribute to additional image noise.

The high voltage bias field is applied between the TFT ground plane and the upper electrode of the detector (Figure 1). With direct contact of metal to the selenium, under the strong field of the high voltage potential, electrons can be injected from the negative terminal to the selenium layer and holes can be injected from the positive terminal even in the absence of light or x-ray photons (8). In addition, when the high voltage is turned on, changed, or reversed, a transit current is observed from the alignment of the internal field to the applied potential. Both the charge injection and the transit of internal electric field will appear as an external current with charges accumulated in the pixel storage capacitors. While the magnitude of these currents are mostly repeatable in a given panel structure or a

Medical Imaging 2010: Physics of Medical Imaging, edited by Ehsan Samei, Norbert J. Pelc,
Proc. of SPIE Vol. 7622, 762218 · © 2010 SPIE · CCC code: 1605-7422/10/$18 · doi: 10.1117/12.845279

constant field changing sequence, these current also contain a noise component that is not repeatable. For a given number of electrons accumulated in the pixel storage capacitor, the noise follows Poisson's statistics and is equal to the square root of the number of electrons from these currents.

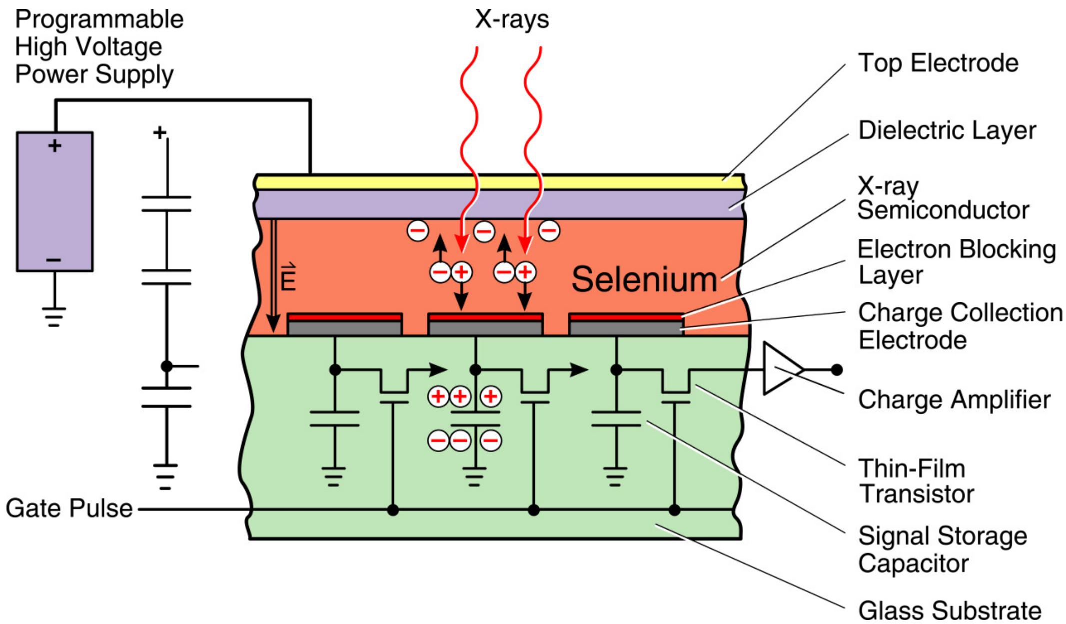

Figure 1. Layer structure of a selenium-TFT imaging detector

2. BLOCKING LAYERS

To minimize the charge injection, an electron blocking layer is required at the negative high voltage electrode/selenium interface, and on the opposite side of the selenium layer, holes blocking layer at the positive electrode/selenium interface. A number of blocking methods have been published (9) and are well known. A typical example is as follows. Consider an arsenate doped selenium detector using positive voltage bias on the upper electrode. Due to fractionation during thermal evaporation of selenium in the deposition process, the bottom layer of the selenium layer contains a higher percentage of arsenate atoms and becomes more p-type. Upon the onset of applied bias, the electrons initially injected into this layer will quickly occupy the p-sites and produce an electron barrier to stop most of the further injection. On the opposite side of the selenium layer, an n-type selenium layer can be deposited to capture the initially injected holes. The electric field from the captured holes will minimize further holes injection. Table 1 is taken from Kasap et al (9). A number of leakage currents from different blocking structures are listed. The leakage current (dark current from charge injection) ranges from the order of 10pA/mm^2 to less than 1pA/mm^2. Recently, G. Zentai (10) has reported a dark current of less than 0.3 pA/mm^2 from selenium sample deposited by Hamamatsu (11), and FujiFilm (12) of Japan has reported leakage current as low as 0.1 pA/mm^2.

For an x-ray exposure window Δt, the total number of electrons accumulated in the pixel electrode from this leakage current (dark current), J_d is : ($J_d A\ \Delta t/e$) where the unit of J_d is coulomb/second (ampere), A is the pixel area, and e is the electronic charge (1.6E-19 coulomb). The stochastic Poisson noise is therefore $(J_d A \Delta t/e)^{1/2}$. For a selenium detector with storage capacitor C, the number of electrons in thermal noise arising from the ground level quantum energy is: $(KTC)^{1/2}/e$.

For C = 1 pf, and T=300, $\qquad (KTC)^{1/2} = 402$ e

Photoconductor, state, preparation	**F V/um**	**I_d pA/mm^2**
Stabilized a-Se Single layer	~ 10	< 10 up to 10 V/μm field
Stabilized a-Se, Multi layer (PIN or NIP)	~10	< 1 up to 20V/μm field
HgI2 Polycrystalline PVD	~ 0.5	~ 6 at 0.5 V/μm field
HgI2 Polycrystalline SP	~ 1.0	~8 at 1.0 V/μm field
$Cd_{.95}Zn_{.05}Te$ Polycrystalline	~0.25	~25 at 0.25 V/μm field
PbI_2 Polycrystalline PVD	~ 0.5	10-50 at 0.5 V/μm field
PbO Polycrystalline	~1.0	40 at 3 V/μm field

Table 1: Dark Current in various potential x-ray photoconductors, (Adapted from S.O. Kasap, G. Belev, Ref 9) Data from Ref 13.

During each readout cycle, when the image charge is transferred to the charge integrating amplifier, this ground level quantum energy will be included. Since the total noise of the image is the square root of the sum of the squares of all the noise components, for the dark current noise not to be a dominating component, it should be no more than the KTC thermal noise. i.e.

$$(J_d A \Delta t/e)^{1/2} < (KTC)^{1/2}/e$$

Typical x-ray windows for medical imaging range from milli-seconds to a few seconds. For an x-ray window of one second, and a detector element size of 139um by 139um,

$$J_d < 2.6\text{x}10^{-14} \text{ Amp/ pixel or } 1.3\text{x}10^{-12} \text{ Amp/mm}^2 \text{ (1.3 pA/mm}^2)$$

For detectors that require very low image noise and very long x-ray window, such as x-ray crystallography, the x-ray window can be as long as 60 seconds for each readout cycle. In this case, the leakage current needs to be one to two orders of magnitude lower.

$$J_d < 4.3\text{x}10^{-16} \text{ Amp/ pixel or } 2.2\text{x}10^{-14} \text{ Amp/mm}^2 \text{ (0.022pA/mm}^2)$$

This level of low dark current can be achieved by using an insolating blocking level as shown in the detector structure of Figure 1. It is also known that directors with direct contact of high voltage electrode with the selenium material, the leakage current in the x-ray irradiated area is higher than it was before the radiation. Safar O. Kasap, and G. Belev stated (9): "The dark current I_d before x-ray generation, and the dark current I_d' after the cessation of x-ray generation, are not the same. In general, I_d' is larger than I_d, and also decays with time. Over the time scale of the observations, I_d' did not seem to come down to the same level I_d … ". An experiment shown in the figure 2 below also demonstrates this effect. Two 7 cm by 7 cm samples of selenium deposited on ITO substrates, one has a gold HV electrode in direct contact with the upper surface and the second one has a 20um of Parylene blocking interface between the Chromium HV electrode and the selenium. A potential of 2,000 volts is applied to the HV electrode and a 20 G ohm ($2\text{X}10^{10}$ ohms) resistor is connected between the ITO substrate and the ground return of the HV power supply. The potential of the ITO is measured with a non-contact electro-static probe and plotted in time after HV is applied followed by periodic x-ray radiation. The sample with direct contact shows a decreasing leakage current passing through the 20 G ohm resistor with leakage increasing after each x-ray irradiation. The leakage current of the sample with an insulating layer (Parylene) shows a much lower leakage current. After each x-ray irradiation, the current also returns to a low leakage value in a much shorter time. However, it is also obvious that the current generated by the successive x-ray pulse decreases gradually after each x-ray exposure. This is due to the build up of counter charges trapped at the insulator/selenium interface. In an imaging detector, these trapped charges at the interface must be removed to restore the x-ray sensitivity before the next x-ray exposure.

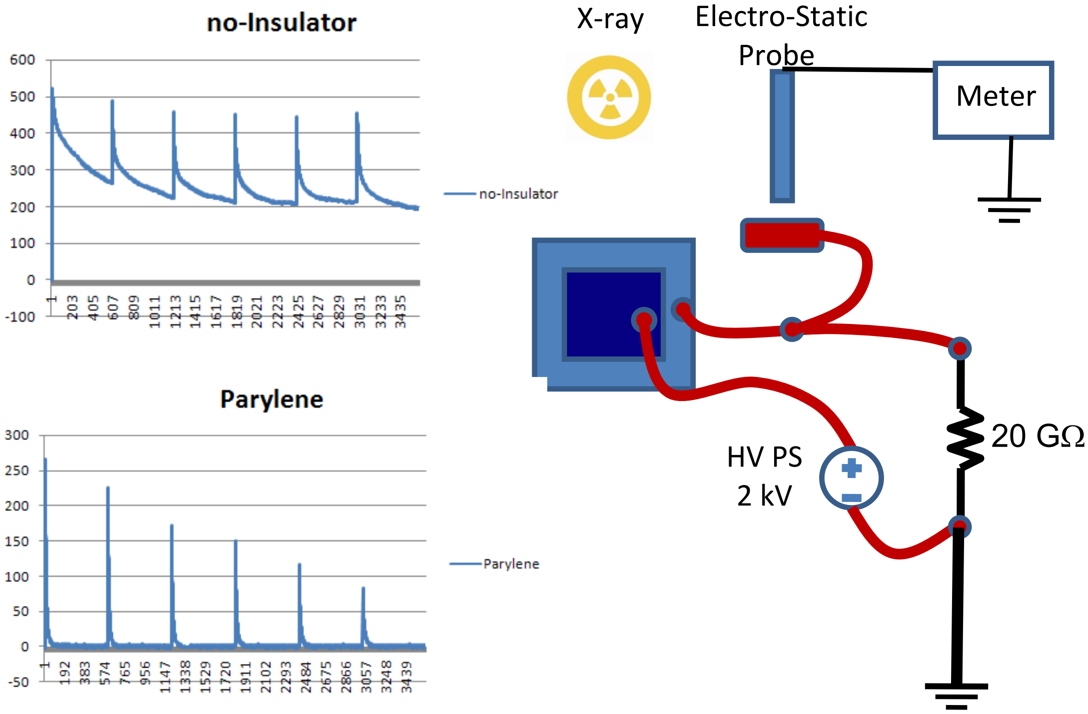

Figure 2: Experiment set up for the measurement of leakage current

The increase of leakage current at the radiated area is highly undesirable for ghosting in medical imaging and can produce large errors the diffraction dot intensity measurement in x-ray crystallography. For selenium panel using an insulating material as blocking layer (such as Parylene), the leakage current can be kept to a minimum and not be increased after detection of dots. However, for a detector with an insulating blocking layer, counter charges after x radiation will be trapped at the interface between the selenium and the insulator and must be removed. These charges can return through the bulk of the selenium layer by the reversal of the bias field. The effectiveness of the return of charges can be increased with the addition of light during the erase cycle from the top, bottom or from both. This kind of erase mechanism has the drawback of promoting the instability of the detector. Since the intrinsic resistance of selenium is very high, the settling time of the internal field after the reversal of the bias potential can be on the order of minutes. When the panel is illuminated by light, additional charge pairs are generated and will travel across the panel. These additional charges may increase the number of undesirable trap charges in the panel after the erase cycle.

3. A NEW METHOD FOR TRAPPED CHARGE REMOVAL

A new method is now being investigated. Two “gutter” electrodes are deposited on the edges of the two side of the upper selenium surface. These electrodes are electrically in direct contact to the selenium layer. A thin layer of dielectric material is then deposited to cover both the gutter electrodes and the overall selenium upper surface. Three or more groups of strip electrodes parallel to the gutter electrodes are than deposited over the entire detector surface including overlapping areas with the gutter electrodes. Every three (or more) strip electrodes are connected together as shown in Figure 3.

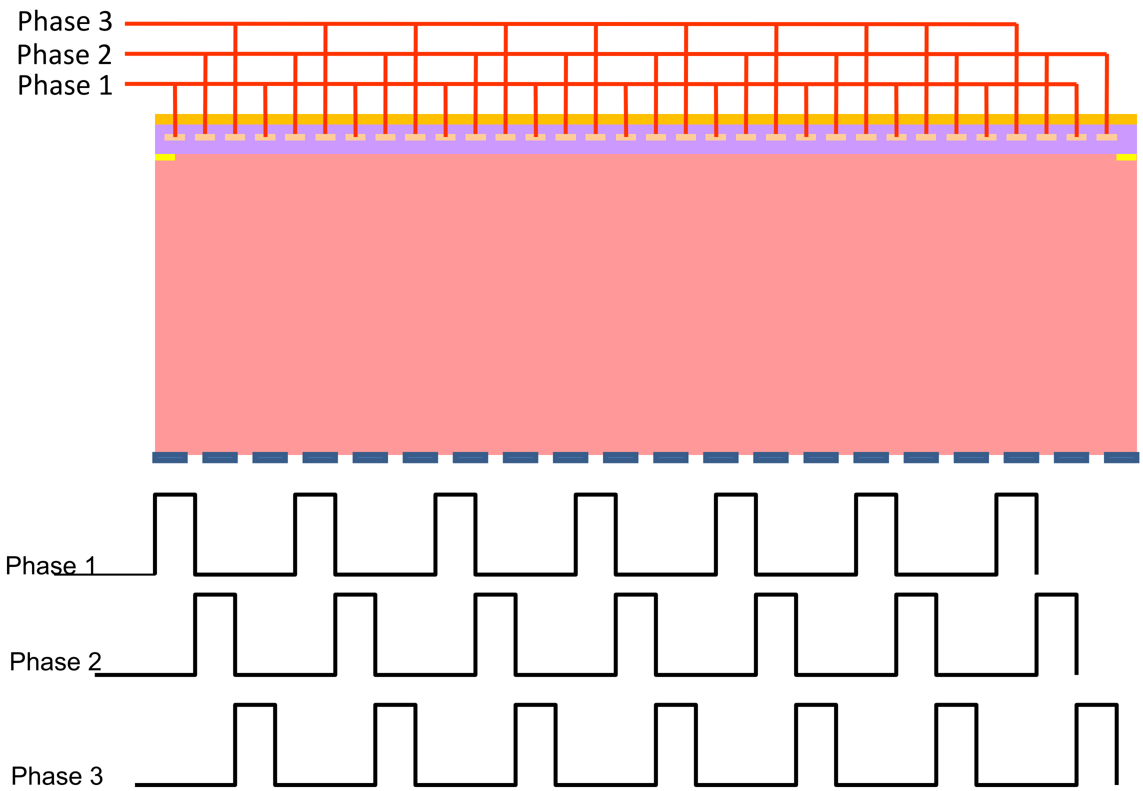

Figure 3: detector layer structure with gutter electrodes and strip electrodes

The high voltage electrode will then be deposited with another thin layer of dielectric material separating the HV electrode and the strip electrodes. When the high voltage bias is applied to the panel, a slightly lower potential corresponding to the potential at the layer position of the strip electrodes without these electrodes is also applied to the strip electrodes. The electric field across the detector is therefore unperturbed by the presence of the strip electrodes before the detection of radiation. After exposure to the x rays, and the readout of the image information, a series of three-phase electrical pulses are then applied to the strip electrodes. These pulses will modulate the baseline voltage of the strip electrodes with each group having a time shift relative to the adjacent electrode as shown in Figure 4. The wave shape of these pulses can be square pulses, sinusoidal waves or triangular waves with three (or more) time phases between the adjacent strips. Simulation of this arrangement has shown a propagating field along the selenium/dielectric interface with field strength proportional to amplitude of the modulating pulses or waves. Figures 5 to Figure 10 shows the propagating potential (PHI) at the interface. Figures 11 to 16 show the propagating lateral electric field (Ey) during the peak of each phase.

This simulation was done with a modulation of 100 volts. With the typical charge transport properties of amorphous selenium of 0.13 cm^2/volts-sec for holes and $1.8x10^{-4}$ cm^2/volts-sec for electrons, a lateral electrical field of 1 volt/mm can drift the holes along the surface with the velocity of 1300 cm/sec and the electrons with the velocity of 35 cm/sec. Higher modulation will result in high lateral fields and therefore faster transit times between strips.

We are now in the process of preparing small samples of selenium plates for further investigation and also preparing full size imaging panel for testing.

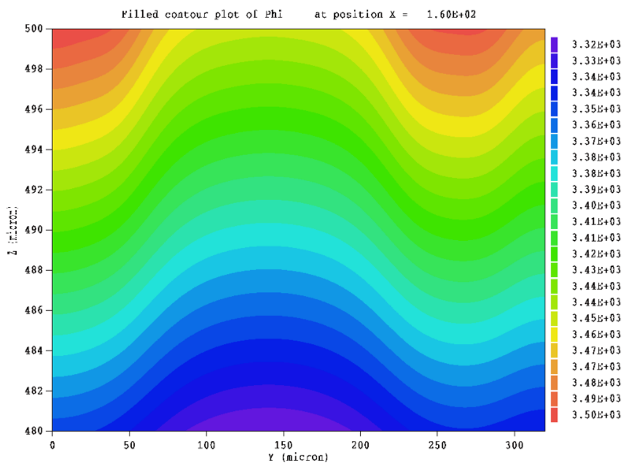

Figure 5: T=1 PHI

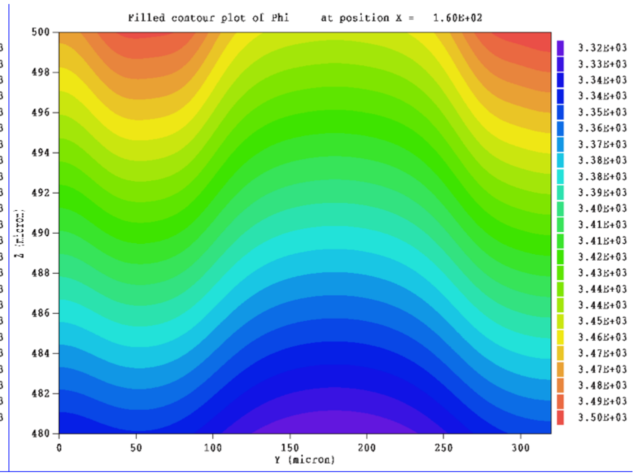

Figure 6: T=2 PHI

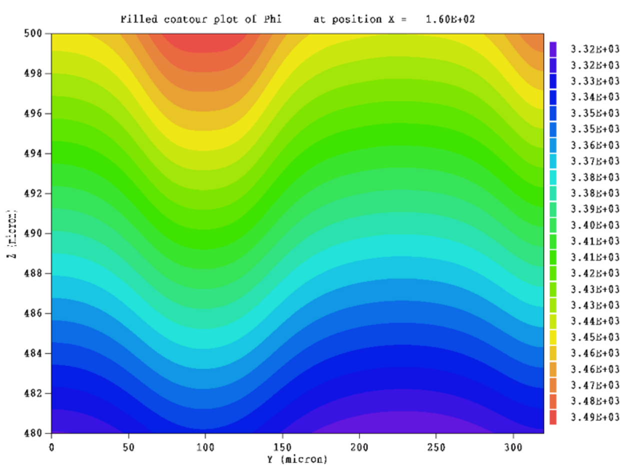

Figure 7: T=3PHI

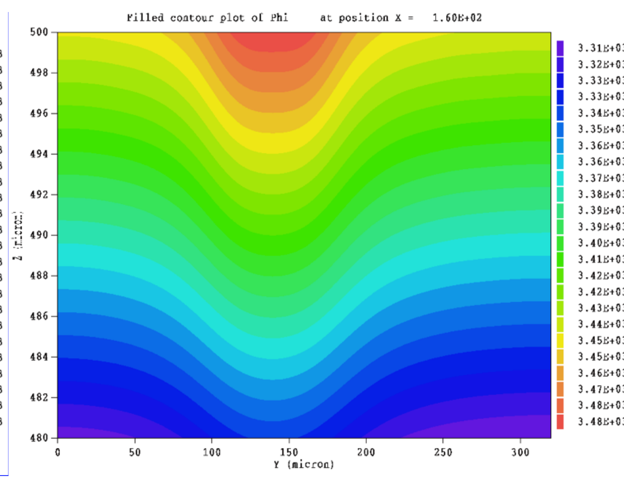

Figure 8: T=4 PHI

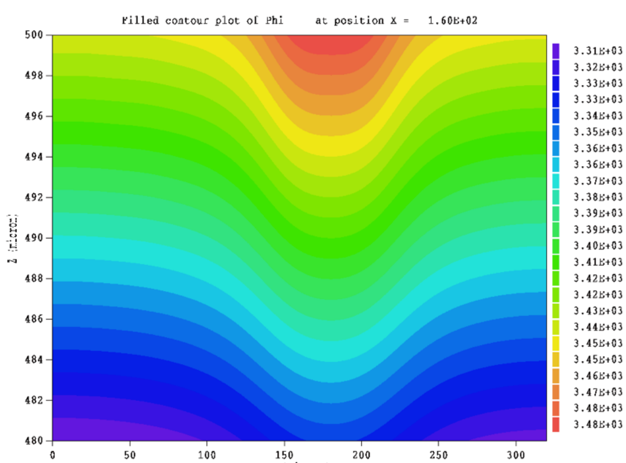

Figure 9: T=5 PHI

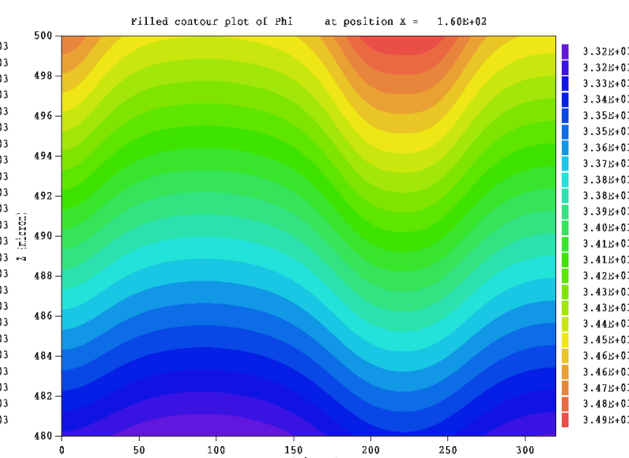

Figure 10: T=6 PHI

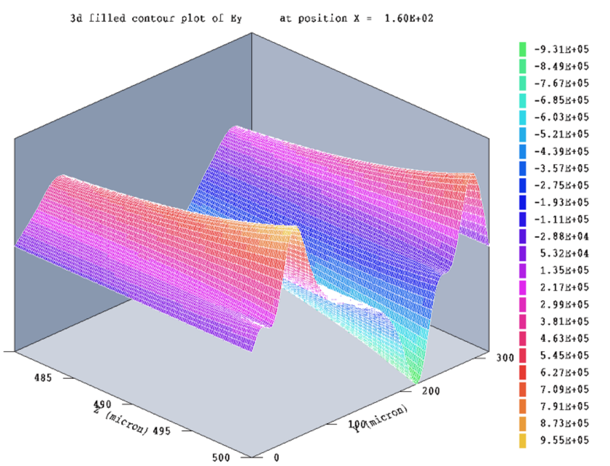

Figure 11: T=1 Ey

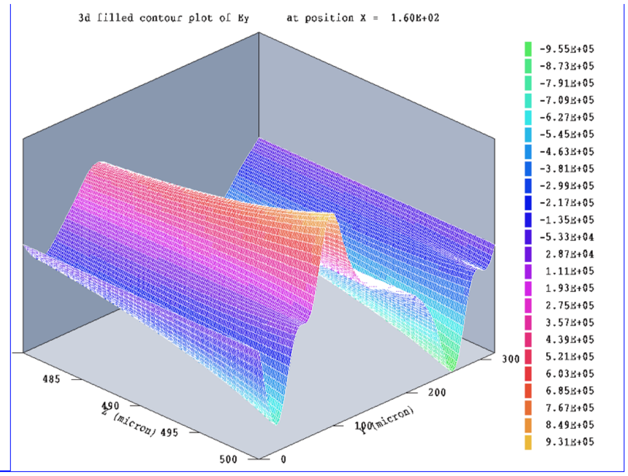

Figure 12: T=2 Ey

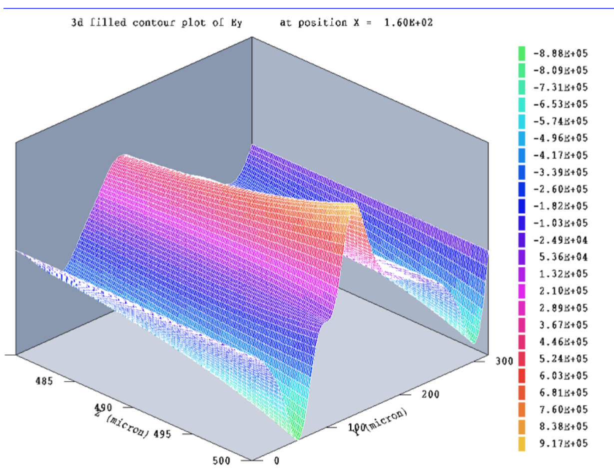

Figure 13: Ey

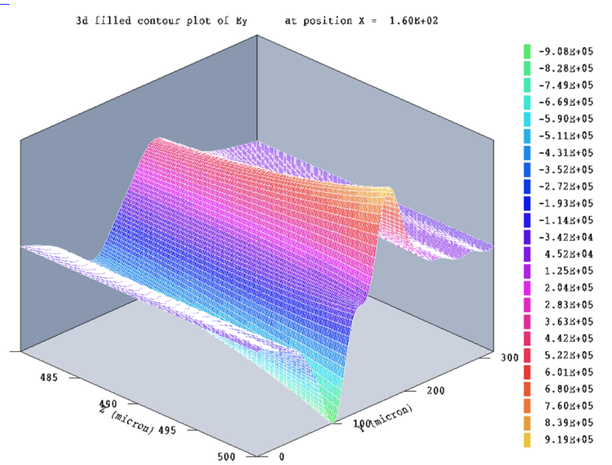

Figure 14: Ey

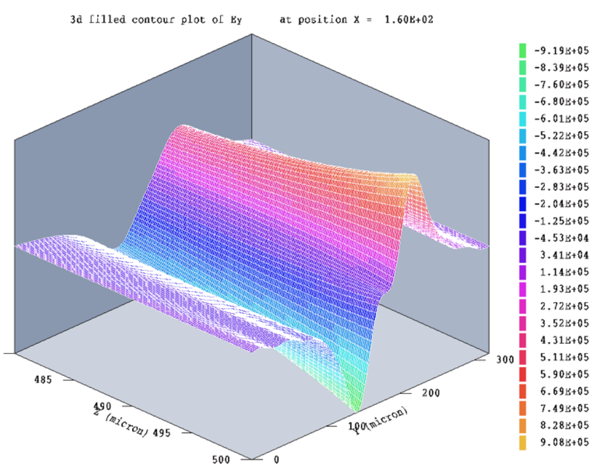

Figure 15: Ey

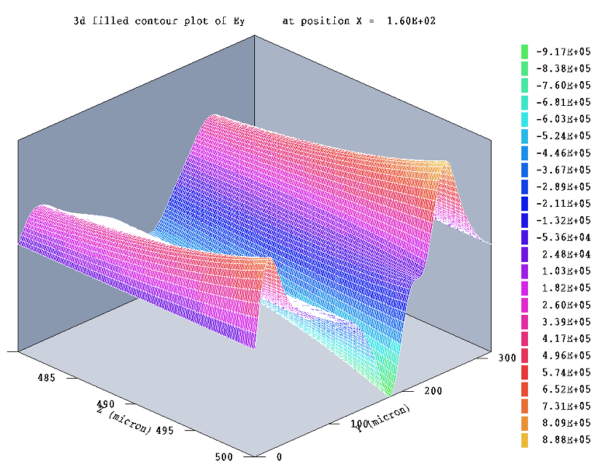

Figure 16: Ey

ACKNOWLEDGEMENTS

This research is supported by a grant from the National Institutes of Health (Grant R43 EB009553). The contents of this paper are solely the responsibility of the authors and do not necessarily represent the official views of the National Institutes of Health or the National Institute of Biomedical Imaging and Bioengineering.

REFERENCES

1. D.L. Lee, L.K. Cheung, and L.S. Jeromin, "A new digital detector for projection radiography", Proc. SPIE, Vol. 2432, pp237-249. (1995); U.S. Patent 5,319,206 (1994)
2. G.S. Shaber, D.L.Lee, J. Bell, G. Powell, and A.D.A. Maidment "Clinical Evaluation of a full field projection radiography detector" Proc. SPIE Vol. 3336, pp. 463-469 (1998)
3. D.L. Lee, L.K. Chang, E.F. Palecki and L.S. Jeromin, "A discussion on Resolution and Dynamic Range of Se-TFT Direct Digital Radiographic Detector", Proc. SPIE Vol. 2708, pp. 511-522 (1996)
4. J.G. Yorker, L.S. Jeromin, D.L. Lee, E.F. Palecki, K.P. Golden, Z. Jing, "Characterization of a Full Field Digital Mammography Detector based on direct x-ray conversion in Selenium" Proc. SPIE Vol. 4682, pp.21-29 (2002)
5. S.O. Kasap, and J.A. Rowlands, Proc. IEEE 90, (2002), 591.
6. G. Belev, S. Kasap, J.A. Rowlands, D. Hunter, M. Yaffe " Dependence of the electrical properties of stabilized a-Se on the preparation conditions and the development of a double layer x-ray detector structure" Applied Physics, 8, (2008) 383-387.
7. Safa O. Kasap, Chris Haugen, Mark Nesdoly, John A. Rowlands "Properties of a-Se for use in a flat panel X-ray image detectors" Journal of Non-Crystalline Solids 266±269 (2000)
8. R.E. Johanson, S.O. Kasap, J. Rowlands, B. Polischuk "Metallic electrical contacts to stabilized amorphous selenium for use in x-ray image detectors" Journal of Non-Crystalline Solids, 227-230, Z1998, 1359-1362.
9. S.O. Kasap, G. Belev, "Progress in the science and technology of direct conversion x-ray image detectors: The development of a double layer a-Se based detector" Journal of Optoelectronics and Advanced Materials Vol. 9, No. 1, January 2007, p.1-10
10. G. Zentai, L. Partain, M.Richmond, K.Ogusu, S.Yamada, SPIE Medical Imaging Conference, presentation number 7622-40, (2010)
11. K.Ogusu, O. Nakane, Y.Igasaki, Y.Okamura, S.Yamada, T.Hirai, "Advanced a-Se film with high sensitivity and heat resistance for x-ray detectors" Proc. Of SPIE Vol. 7258, pages 72583M-1 to 10.
12. F.Nariyuki, S.Imai, H.Watano, T.Nabeta, Y.Hosoi, SPIE Medical Imaging Conference, poster paper number 7622-144, (2010)
13. M.Z.Kabir, S.O.Kasap, J.A.Rowlands, in Springer Handbook of Electronic and Photonic Materials, Ed. Safa Kasap and Peter Capper, Springer, Heidelberg (2006), Ch. 48.